Journal of Physiology (1991), **442**, *pp.* 47–64
With 7 figures
Printed in Great Britain

HUMAN PERIPHERAL SPATIAL RESOLUTION FOR ACHROMATIC AND CHROMATIC STIMULI: LIMITS IMPOSED BY OPTICAL AND RETINAL FACTORS

BY STEPHEN J. ANDERSON*, KATHY T. MULLEN† AND ROBERT F. HESS†

*From *The Physiological Laboratory, Downing Street, Cambridge CB2 3EG and the †McGill Vision Research Centre, Department of Ophthalmology, 687 Pine Avenue West, H4-14, Montreal, Quebec, Canada H3A 1A1*

(*Received 2 October 1990*)

SUMMARY

1. The aim of this study was to determine whether optical, receptoral or higher-order neural properties limit spatial resolution (acuity) in human vision, especially in the peripheral regions of the visual field.

2. Both achromatic and chromatic stimuli were used, and measures were taken to ensure that the resolution estimates were not contaminated by the detection of spatial sampling artifacts. Spatial contrast sensitivity functions were measured at retinal locations from 0 to 55 deg along the naso-temporal meridian for: (i) discriminating the direction of drift of luminance-modulated (black–white) sinusoidal stimuli drifting at 8 Hz (achromatic task); and (ii) for detecting isoluminant red–green sinusoidal stimuli drifting at 0·4 Hz (chromatic task). Achromatic contrast sensitivity functions were also measured along the vertical meridian for eccentricities of 8 and 40 deg. Each achromatic function was extrapolated to a contrast sensitivity of one (100% contrast) to estimate achromatic acuity. Chromatic acuities were obtained by expressing chromatic contrast in terms of cone contrasts and using the same method of extrapolation. We compared the results with recent data on *human* optical properties and retinal anatomy.

3. Both achromatic and chromatic acuity decline with distance from the fovea, but at a faster rate than that dictated by the known optical and/or receptoral properties of the human eye. We conclude that, for stimuli of either achromatic or chromatic contrast, peripheral spatial resolution is limited by post-receptoral mechanisms. Also, chromatic acuity declines more steeply than luminance acuity with eccentricity suggesting that there are additional post-receptoral limitations on colour resolution in the periphery.

4. A clear naso-temporal asymmetry is seen in the resolution whose dependence is qualitatively, but not quantitatively, similar to the Nyquist limits imposed by the asymmetric density of human retinal ganglion cells. We discuss the possibility that

* To whom correspondence should be addressed at The Department of Vision Sciences, Aston University, Aston Triangle, Birmingham B4 7ET.

MS 8834

in peripheral vision (beyond the optic nerve head) the spacing of ganglion cells may pose a fundamental limit on the resolution of achromatic stimuli, but not chromatic stimuli.

INTRODUCTION

Visual resolution has long been regarded as one of the key measures of visual performance and since the original work of Wertheim (1894) its dependence on eccentricity has been the subject of many studies (e.g. Low, 1951). More recently, interest has been developing in the processes which underlie the variation of visual resolution with eccentricity.

It is now clear that optical and receptoral properties play a major role in limiting human foveal vision (Campbell & Gubisch, 1966; French, Snyder & Stavenga, 1977; Williams, 1985; Banks, Geisler & Bennett, 1987). Spatial resolution for achromatic stimuli reaches 60 cycles deg^{-1} in the fovea, which approximates the acuity limit dictated by the sampling limitations of the cone mosaic and optical blurring (e.g. Williams, 1985; Banks *et al.* 1987). Also, there is evidence that receptoral sampling limits spatial resolution for some chromatic stimuli. Specifically, the central acuity of the short-wavelength-sensitive (S) cone mechanisms may be limited by receptoral sampling, since measured unaliased acuities of S cones approximate the limit expected from their sparse distribution (Williams, Collier & Thompson, 1983; Hess, Mullen & Zrenner, 1989). On the other hand, measures of chromatic acuities based on medium- and long-wavelength-sensitive (M and L) cones fall below the receptoral sampling limitations, suggesting that post-receptoral factors limit foveal resolution for some chromatic stimuli (see Discussion for further details).

It is less clear which factors limit peripheral vision. Several 'front-end' properties of the primate visual system vary with eccentricity, including: optical quality (Jennings & Charman, 1981), cone aperture size (Polyak, 1957), cone density (Osterberg, 1935; Curcio, Sloan, Kalina & Hendrickson, 1990), ganglion cell density (e.g. Perry, Oehler & Cowey, 1984) and the spatial frequency transfer characteristics of ganglion cells (Crook, Lange-Malecki, Lee & Valberg, 1988). These properties do not all vary in unison and peripheral spatial resolution may in principle be limited by any or none of them.

An accurate assessment of how spatial resolution and the 'front-end' properties of the human visual system vary with retinal eccentricity has been hampered for two reasons. First, there has not been adequate optical and anatomical data available for human eyes to make this assessment and so previous studies have relied on monkey data (e.g. Thibos, Cheney & Walsh, 1987*a*; Merigan & Katz, 1990). Second, the human peripheral retina is subject to sampling artifacts or aliasing (e.g. Smith & Cass, 1987; Thibos, Walsh & Cheney, 1987*b*) and detection of these artifacts may result in spuriously high estimates of spatial resolution. Perhaps the clearest evidence for aliasing comes from studies using drifting periodic stimuli to measure spatial resolution. Coletta, Williams & Tiana (1990) provide evidence for receptoral undersampling in human peripheral vision using drifting interference fringes imaged directly on the retina: for spatial frequencies beyond the cone sampling limit, the fringes appear to move in the opposite direction from their true direction of motion. This 'reverse motion phenomenon' is a consequence of spatial undersampling and

allows a clear distinction between aliased and non-aliased measures of acuity (see also Gotz, 1964). Anderson & Hess (1990) showed that even under normal viewing conditions reverse motion phenomena occur in human peripheral vision.

Only measures of visual resolution that remain uncontaminated by the detection of any aliased components can provide information about the sampling density of the limiting mosaic. This information can then be usefully compared with anatomical and physiological estimates of neural densities.

In this paper we describe the eccentricity dependence of both achromatic and chromatic spatial resolution under normal viewing conditions, and compare the results with recent data on human optical and retinal properties. To do so, we employ methods that provide a measure of acuity that is free from sampling artifacts so that the density of the underlying sampling array can be estimated. Both achromatic and chromatic stimuli were used as the processing of these stimuli may involve different visual mechanisms (e.g. Zeki, 1978; Lennie & D'Zmura, 1988). We assess the dependence of each of these spatial acuities with retinal eccentricity in order to distinguish whether their major limitation is from optical, receptoral or post-receptoral sources.

METHODS

Experiment I: *achromatic stimuli*

Stimuli were generated by computer and displayed on a Joyce Electronics cathode ray tube (CRT; model DM2, P4 phosphor) using a standard raster technique. The CRT was linear up to 95% contrast (defined as $L_{max}-L_{min}/L_{max}+L_{min}$, where L is luminance) and this value was never exceeded. For Expt I, the display screen had a mean luminance of 225 cd m^{-2} and was delimited by a 20 cm diameter circle cut in a 2·0 m white cardboard surround, illuminated to the same mean luminance as the screen. A small black central or eccentric fixation spot was used. Retinal eccentricity (e) was measured from the centre of the stimulus.

The stimulus was a drifting vertical sine wave grating, Gaussian damped in two-dimensional space ($\sigma_x = \sigma_y$ and was: 0·23 deg for foveal viewing; 0·29 deg for $e = 4$ deg; 0·5 deg for $e = 8$ deg; 1·26 deg for $e = 16·5$ deg; and 2·5 deg for $e = 25$, 32·5, 40, 47·5 and 55 deg). Stimuli were damped in time using a raised cosine envelope (one period was 1000 ms). The grating drifted either to the left or right with a temporal frequency of 8 Hz. Direction of drift was randomized between trials. Spatial frequency was varied by altering the optical viewing distance and/or changing the number of cycles on the display screen. For measurements used to estimate spatial resolution, the minimum number of spatial cycles displayed in $2\sigma_x$ was 2·5 cycles, which exceeds the critical summation area (of about 1·0 cycle) for drifting (8 Hz) sine wave gratings (Anderson & Burr, 1987), thus avoiding the influence of stimulus size on contrast thresholds.

For all measurements, the criterion for threshold was the minimum contrast at which the direction of drift (right or left) or the test grating could be seen. Stimulus contrast was adjusted to threshold using a two-up–one-down staircase procedure with ten reversals. Each datum is the mean of at least three separate threshold determinations. Contrast sensitivity was defined as the reciprocal of threshold contrast.

Experiment II: *chromatic stimuli*

Sine wave stimuli were displayed on two Joyce screens (model DM2, each with a white P4 phosphor), viewed separately through narrow-band interference filters (with peak transmission at 526 and 602 nm) to produced their colour, and combined optically 180 deg out of phase to form the composite red–green grating (see Mullen, 1985 for details). The full bandwidth (at half-height) of each interference filter was 22 nm. Contrast (C) of each component luminance grating was defined as Michelson contrast and the contrasts of the two component gratings were always equal to each other, although their respective mean luminances may differ. Chromatic contrast was defined as the contrast of either component grating. The mean luminance of the combined display was

constant at 42 cd m^{-2}. The fixation target was small black spot affixed to the CRT screen for central viewing and a white LED (light-emitting diode) affixed to a cardboard surround for eccentric viewing.

Following Mullen (1985), we corrected for the chromatic difference of magnification of the eye at all spatial frequencies by adjusting the spatial frequency of one of the component gratings for foveally viewed, unity contrast square-wave stimuli. The gratings were displayed horizontally to further reduce the effects of any residual chromatic difference of magnification for stimuli eccentrically imaged along the horizontal meridian. For foveal and parafoveal ($e = 2{\cdot}5$ deg) stimuli, the chromatic difference of focus was also corrected (Mullen, 1985). At greater eccentricities, the chromatic difference of focus could not be corrected without a risk of introducing further aberrations.

The chromatic grating patch was circular and hard-edged, with a diameter of : 0·28 deg for $e =$ 0 and 2·5 deg; 1·36 deg for $e = 5$ deg; 2·5 deg for $e = 8$ deg; 5·0 deg for $e = 16$ deg; and 7·5 deg for $e = 25$ and 30 deg. Viewing distance was fixed at 82 cm: spatial frequency was varied by changing the number of cycles on the display screens. For measurements used to estimate chromatic spatial resolution a minimum of 1·0 cycle was displayed in order to avoid any significant influence of stimulus size on chromatic contrast thresholds (see Mullen, 1991). For eccentricities of 0 and 2·5 deg, a Zeiss 3 × telescope was used in reverse to achieve high spatial frequencies. The gratings drifted up with a temporal frequency of 0·4 Hz. A bite bar was used to align the observer's head.

The criterion was detection of chromatic (red–green) bars. To meet this criterion, and to ensure that threshold estimates were not affected by the detection of any luminance artifacts, chromatic contrast was adjusted to threshold using method of adjustment. Each datum is the mean of at least three runs. Contrast sensitivity was defined as the reciprocal of chromatic contrast.

For Expts I and II, observers monocularly viewed the fixation mark, were refracted for distance vision and used natural pupils and accommodation. If Troxler's effect (the progressive dimming of objects in the periphery of the visual field under steady fixation) was experienced, fixation was averted to allow time for recovery. Data are reported for three observers: the corrected Snellen acuity of each is 6/6, and each has normal visual fields and normal colour vision. All observers have received considerable practice in setting both achromatic and chromatic contrast thresholds.

RESULTS

Experiment I: achromatic stimuli

In this experiment our principal aim was to determine achromatic spatial resolution across the retina. We began by measuring the spatial contrast sensitivity function at each eccentricity. For each set of measurements, the data points associated with the high-frequency decline in sensitivity were fitted with an exponential function, which was extrapolated to a contrast sensitivity of one (100% contrast) to predict acuity (e.g. Robson, 1966). To ensure that our acuity estimates were not affected by the detection of any aliased components, we chose direction discrimination as our criterion for threshold for drifting sinusoidal stimuli (see Introduction). The drift rate was 8 Hz, which is near optimal for achromatic contrast sensitivity for a wide range of spatial frequencies (Robson, 1966; Burr & Ross, 1982).

Data were collected for two observers (S.A. and R.H.) for retinal eccentricities from 0 to 55 deg along the nasal and temporal meridia. Figure 1 shows representative results for observer S.A. at eccentricities of 8, 25, 40 and 55 deg. The results for R.H. were similar. Note that when plotted on logarithmic co-ordinates the data points associated with the high-frequency roll-off in contrast sensitivity can be adequately fitted by an exponential function (continuous line through data).

In the near periphery, at 8 deg eccentricity, there is no naso-temporal asymmetry in contrast sensitivity to gratings of any spatial frequency, including those near the acuity limit. The functions are low-pass on log–log co-ordinates with peak sensitivity

of about 300 at spatial frequencies up to 3·0 cycles deg^{-1}, and thereafter decline rapidly reaching an acuity limit of around 10·0 cycles deg^{-1}.

In the far periphery from 25 to 55 deg, both contrast sensitivity and acuity decline, as expected (Robson & Graham, 1981). Also, there is a clear naso-temporal

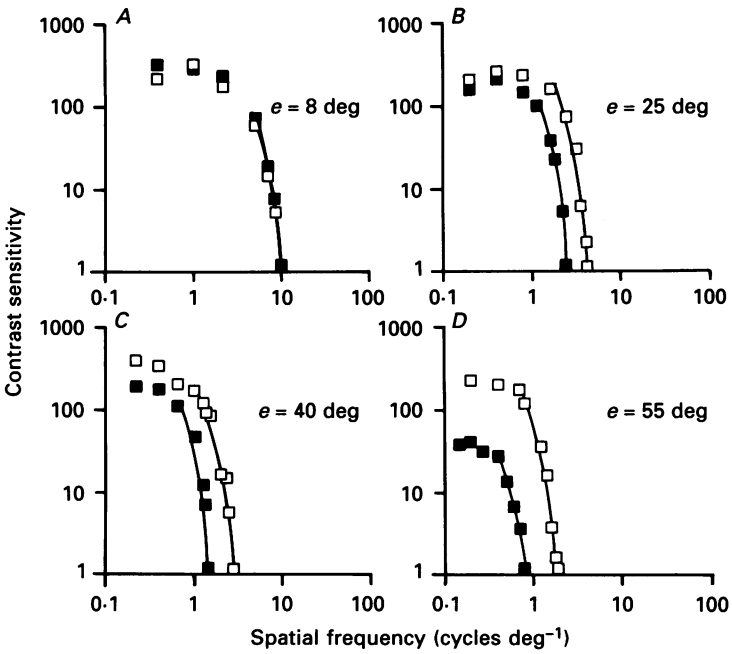

Fig. 1. Measurements of contrast sensitivity for discriminating the direction of drift (right or left) of luminance-modulated (black–white) sinusoidal stimuli drifting at 8 Hz as a function of stimulus spatial frequency. The results are for observer S.A. for eccentricities (e) of 8, 25, 40 and 55 deg (panels *A–D* respectively) along the horizontal meridian. The method of extrapolation used to predict acuity is described in the text. □, nasal retina; ■, temporal retina. Symbol sizes were typically 1–2 standard errors of the mean. Note the naso-temporal asymmetry in contrast sensitivity in the far peripheral visual field.

asymmetry in sensitivity: as noted by Wertheim (1894), stimuli imaged on the nasal retina are detected with higher sensitivity than those imaged on the temporal retina. Together with other measurements, we find that this divergence in sensitivity begins at about 20 deg and steadily increases with increasing retinal eccentricity thereafter (see Fig. 5 also). At 55 deg, achromatic acuity is 1·9 cycles deg^{-1} in the nasal retina and 0·8 cycles deg^{-1} in the temporal retina.

This experiment was repeated for peripheral viewing for eccentricities of 8 and 40 deg along the superior and inferior retina. The results, shown in Fig. 2 for observer S.A., indicate that there is no asymmetry in contrast sensitivity along the vertical meridian, even in the far periphery. Along this meridian, acuity declines at a similar rate to that observed in the temporal retina.

Experiment II: chromatic stimuli

The direction discrimination technique could not be used to obtain alias-free measures of chromatic acuity. We attempted this technique but found, as others have done (e.g. Lindsey & Teller, 1990), that it is very difficult to discriminate the

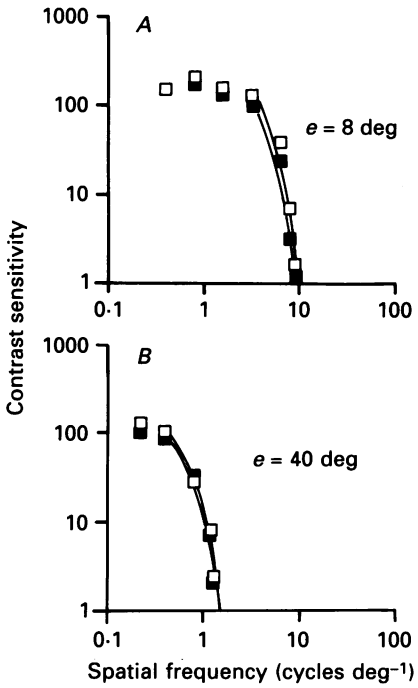

Fig. 2. As for Fig. 1 for retinal eccentricities (e) of 8 and 40 deg (panels A and B respectively) along the vertical meridian. □, superior retina; ■, inferior retina. The results are for observer S.A.

direction of drift of moving isoluminant gratings. At their detection threshold, the direction of drift of chromatic gratings cannot be determined and at higher contrasts they have non-smooth motion. None the less, we found no perceptual evidence of aliasing with stimuli of purely chromatic contrast and return to this issue in the discussion.

To measure chromatic contrast sensitivity, we used isoluminant red–green sinusoidal gratings and a criterion of chromatic detection. We drifted the gratings at 0·4 Hz as this rate is optimal for chromatic contrast sensitivity in both central and peripheral vision (Kelly, 1983; Mullen, 1991).

Stimuli were rendered isoluminant using the method described by Mullen (1985): the ratio of mean luminances of the component colours was varied systematically, and the isoluminant point was defined as the ratio at which a minimum in contrast sensitivity was obtained (i.e. the ratio at which contrast sensitivity for the chromatic grating differed most from the sensitivity for the component monochromatic luminance gratings). The isoluminant point was measured for a range of eccentricities and spatial frequencies. The results showed no evidence for variation in the

isoluminant point with stimulus spatial frequency, although there was some variation with eccentricity. For each subject the measured isoluminant points were used at each eccentricity and are given in the legends to Figs 3 and 4.

Chromatic contrast sensitivity functions

Chromatic contrast sensitivity functions were measured at various retinal locations along the horizontal meridian. The results are shown in Figs 3 and 4 for observers

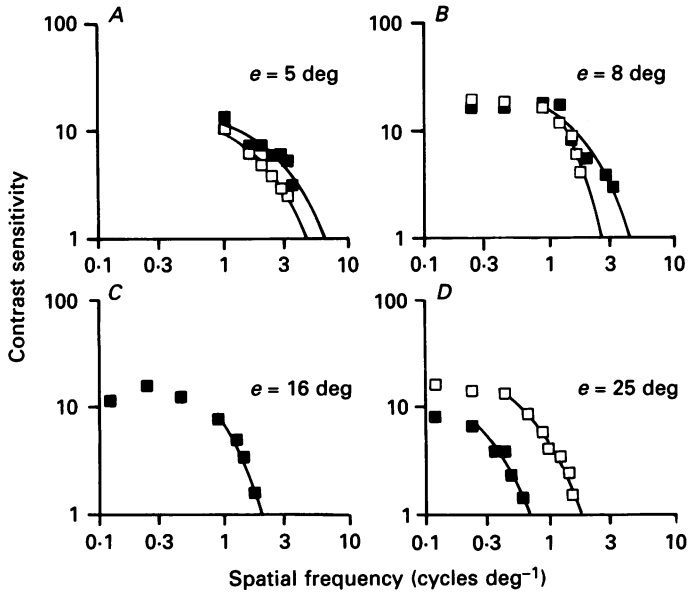

Fig. 3. Measurements of contrast sensitivity to isoluminant red–green sinusoidal stimuli as a function of stimulus spatial frequency for retinal eccentricities (e) of 5, 8, 16, and 25 deg (panels *A–D* respectively) along the nasal (□) and temporal retina (■). The results are for observer S.A. The symbol sizes are approximately 1–2 standard errors of the mean. In the nasal retina, the red/green ratio (r) defining the isoluminant point was 0·52 for eccentricities of 5, 8 and 25 deg. In the temporal retina: $r = 0{\cdot}52$ for $e = 5$ and 8 deg; $r = 0{\cdot}55$ for $e = 16$ deg; and $r = 0{\cdot}57$ for $e = 25$ deg. The continuous line through the data points associated with the high-frequency decline in contrast sensitivity is the fit of an exponential function (see text for explanation).

S.A. and K.M., respectively. To predict the high spatial frequency cut-off, an exponential function was fitted to the data points associated with the high-frequency loss in contrast sensitivity, as for the achromatic results. This allows resolution for the chromatic stimulus (henceforth termed chromatic stimulus resolution) to be measured without using very high-contrast modulations which are more likely to contain detectable luminance artifacts.

Chromatic contrast sensitivity functions when plotted on log–log co-ordinates for both central and peripheral vision are low-pass. Both peak sensitivity and the chromatic stimulus resolution decline with increasing eccentricity, but at different rates in the nasal and temporal retina. In the near periphery for eccentricities from 2·5 to 8 deg, the temporal retina is slightly more sensitive than the nasal retina with

a stimulus resolution about 1·4 times higher than the nasal retina (averaged over all eccentricities and both observers). In the far periphery at 25 and 30 deg eccentricity, the reverse effect occurs and the nasal retina is substantially more sensitive than the temporal retain at all spatial frequencies. At 30 deg, the chromatic stimulus

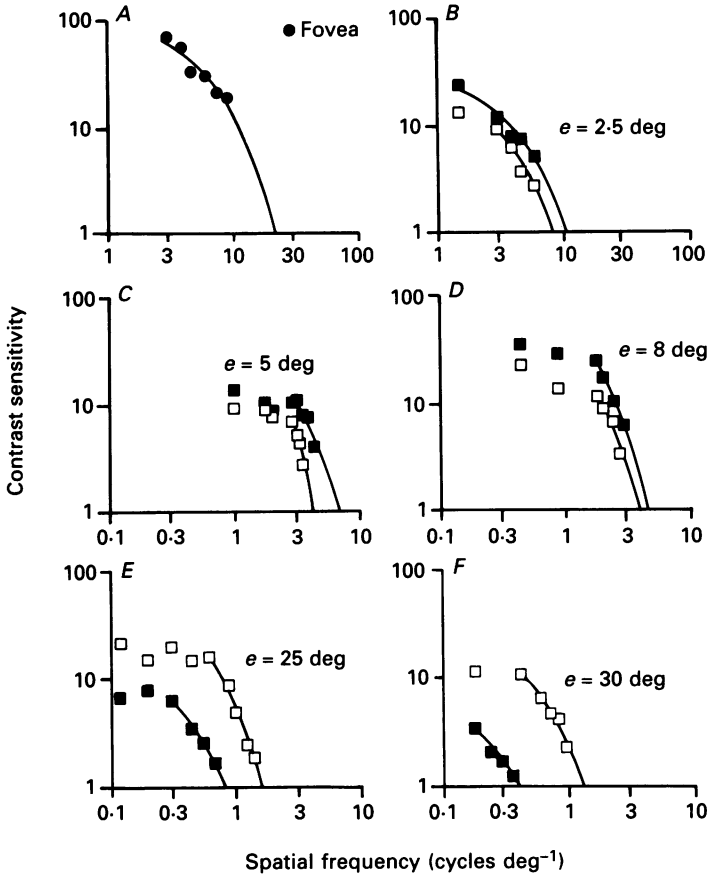

Fig. 4. As for Fig. 3 for observer K.M. for retinal eccentricities from 0 to 30 deg along the nasal (□) and temporal retina (■). The red/green ratio (r) defining the isoluminant point was 0·52 in the fovea. In the nasal retina: $r = 0{\cdot}52$ for $e = 2{\cdot}5$ deg; $r = 0{\cdot}55$ for $e = 5$ deg; $r = 0{\cdot}57$ for $e = 8$ deg; $r = 0{\cdot}55$ for $e = 25$ and 30 deg. In the temporal retina: $r = 0{\cdot}52$ for $e = 2{\cdot}5$ deg; $r = 0{\cdot}55$ for $e = 5$ deg; $r = 0{\cdot}57$ for $e = 8$ deg; and $r = 0{\cdot}60$ for $e = 25$ and 30 deg.

resolution in the nasal retina is 3·4 times greater than for the same eccentricity in the temporal retina (results averaged over both observers).

So far we have expressed colour contrast in terms of the chromatic modulation of the stimulus. This is an arbitrary measure, however, since the measured contrast sensitivity will depend on the colour pair used in the stimulus as well as its modulation. In order to specify an absolute chromatic resolution we adopt a physiologically based measure of colour contrast, in terms of the contrast modulation of the cones produced by the stimulus (termed cone contrast). For each chromatic

contrast sensitivity function, the data were converted to both M- and L-cone contrast sensitivities (see Mullen, 1985), and the resulting functions were then extrapolated in the usual way to a cone contrast sensitivity of unity. The limiting chromatic acuity is given by the lower of the two cut-off frequencies obtained, since it is assumed that both cone types are required for chromatic detection (e.g. Lennie & D'Zmura, 1988). This provides a theoretical resolution limit for chromatic detection (henceforth termed chromatic acuity) that is independent of the colour pair used in the stimulus.

Achromatic and chromatic spatial resolution

From the above measurements we derived achromatic and chromatic spatial acuities at each of the tested eccentricities so that the possible factors underlying these limitations can be assessed.

In Fig. 5 the data symbols show, for two observers, achromatic (square symbols) and chromatic acuity (round symbols) as a function of retinal eccentricity along the horizontal meridian. Note that the chromatic acuities obtained from the extrapolation of cone contrasts are not very much greater (15–25%) than the measured chromatic stimulus resolutions (from Figs 3 and 4). This reflects the fact that the colour pair used in the stimulus already produce quite a strong differential modulation of the L- and M-cone types.

Figure 5 shows that the decline in achromatic acuity is symmetric about the fovea out to at least 8 deg and thereafter is more rapid for stimuli imaged on the temporal retina than on the nasal retina: it decreases from a peak value of 46·0 cycles deg^{-1} in the fovea to 0·84 and 1·8 cycles deg^{-1} at 55 deg along the temporal and nasal retina, respectively (results averaged over both observers).

The chromatic acuity in the fovea is 26·3 cycles deg^{-1}, which corresponds to a chromatic stimulus resolution of 21·6 cycles deg^{-1} (results for K.M.). The decline in chromatic acuity with increasing retinal eccentricity is also asymmetric about the fovea. For example, at 30 deg eccentricity chromatic acuity is 0·52 cycles deg^{-1} in the temporal retina and 1·61 cycles deg^{-1} in the nasal retina (results averaged over both observers).

Figure 5 also shows the maximum spatial frequency resolution afforded by the optical properties of the human eye (Campbell & Gubisch, 1966; Jennings & Charman, 1981), the maximum resolution predicted from spatial filtering by the human cone aperture (assuming the inner segment to be the effective aperture), and the Nyquist limits calculated from cone (Curcio *et al.* 1990) and ganglion cell densities (Curcio & Allen, 1990) in the human retina. The Nyquist limit is the highest sinusoidal spatial frequency (colour or luminance modulation) that can be reconstructed unambiguously from an array of spatially discrete sampling elements. Details of how these calculations were made are given in the Appendix.

Optical quality reaches 60·0 cycles deg^{-1} in the fovea, remains relatively constant at 50·0 cycles deg^{-1} over the central 30 deg, and thereafter decreases to about 40·0 cycles deg^{-1} at 40 deg. Spatial filtering by a single cone aperture (inner segment) limits resolution to 152·0 cycles deg^{-1} in the fovea and approximates the optical limit in the periphery (at least from 10 to 40 deg). The cone Nyquist limit decreases symmetrically about the fovea from a peak value of 57·7 cycles deg^{-1} and reaches

an asymptote of about 10·0 cycles deg^{-1} at 25 deg. The Nyquist limit of the population of ganglion cells as a whole steadily declines in an asymmetric fashion about the fovea from a peak value of about 81·6 cycles deg^{-1} to 4·3 and 2·1 cycles deg^{-1} at 55 deg along the nasal and temporal meridian, respectively.

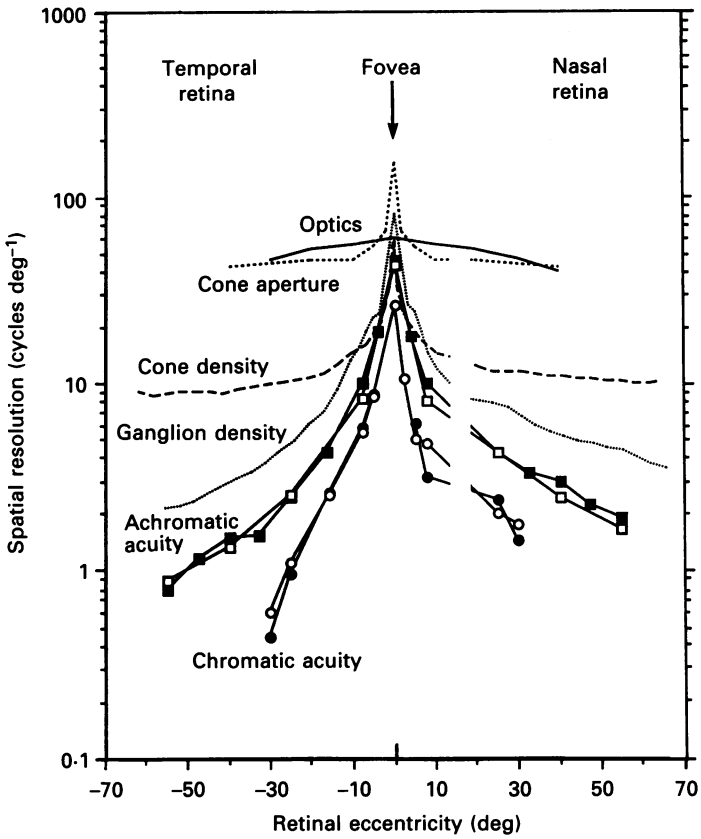

Fig. 5. Psychophysical, optical and anatomical data for the human eye. The data symbols show achromatic acuity (observers S.A. and R.H.; square symbols) and chromatic acuity (observers S.A. and K.M.; round symbols) as a function of retinal eccentricity along the horizontal meridian. The various continuous, dashed and dotted lines show the maximum spatial resolution (cycles deg^{-1}) afforded by: the eye's optical properties (from Campbell & Gubisch, 1966; Jennings & Charman, 1981), the aperture size of individual cones (from C. A. Curcio, personal communication), and the Nyquist limits dictated by cone density (from Curcio *et al.* 1990) and ganglion cell density (from Curcio & Allen, 1990). The Appendix details how these calculations were made.

Figure 5 shows that in human peripheral vision both achromatic and chromatic acuity fall below the limits imposed by the optical and/or receptoral properties of the human eye. They are also less than the Nyquist limit for the population of ganglion cells as a whole. There is some qualitative agreement with ganglion cell density as the spatial resolution limits are asymmetric only in the far periphery (beyond the optic

nerve head), and this is the region where the degree of naso-temporal asymmetry in ganglion cell density becomes significant.

At all eccentricities, chromatic acuity is less than achromatic acuity (Fig. 5). Note also that in both the nasal and temporal retina, chromatic acuity falls two to three times more rapidly with eccentricity than does achromatic acuity. The sites at which visual performance for both achromatic and chromatic stimuli may be limited are discussed in more detail below.

DISCUSSION

Our aim in this study was to ascertain whether optical, receptoral or higher-order neural properties limit spatial resolution in human peripheral vision. We measured the eccentricity-dependent variations in achromatic and chromatic spatial resolution and compared these measures to the limitations imposed by the 'front-end' properties of the human visual system. Our main findings are shown in Fig. 5. Both achromatic and chromatic acuity decline with distance from the fovea, but at a faster rate and in a way that cannot be ascribed to the known optical and/or receptoral properties of the human eye. We suggest that both achromatic and chromatic acuity are limited by post-receptoral mechanisms in human peripheral vision.

Furthermore, the loss in chromatic acuity with retinal eccentricity is steeper than the loss in achromatic acuity. This is compatible with results showing that the decline in contrast sensitivity with eccentricity is steeper for colour than for luminance gratings (Mullen, 1991). Our results provide evidence to suggest that additional post-receptoral factors limit peripheral chromatic acuity, such as a loss with eccentricity in the number, or strength, of cone-opponent mechanisms.

Assumptions of the study

There were two major assumptions in this study: that our measures of achromatic and chromatic visual acuity are uncontaminated by sampling artifacts (Smith & Cass, 1987; Thibos *et al.* 1987*b*; Anderson & Hess, 1990; Coletta *et al.* 1990); and that the acuity limit provides a measure of the minimum sampling element density of the underlying array.

Achromatic acuity was measured with a direction discrimination rather than a detection protocol to eliminate the use of sampling artifacts as a visual cue (see Introduction). Unfortunately, we could not use this protocol with stimuli of purely chromatic contrast but instead had to rely on the use of a threshold based on chromatic detection (see Results). None the less, we did not perceive any aliasing phenomena with any of the colour stimuli used. We conclude from this observation that, either chromatic stimuli are sufficiently sampled across space at all stages within the visual pathways, or the stimuli that we used were not high enough in spatial frequency to be spatially undersampled.

The achromatic and chromatic resolution limits cannot lend themselves directly to a quantitative measure of the density of the underlying sampling array, unless that array is perfectly regular. However, this is unlikely to be so for any biological discrete imaging system (French *et al.* 1977; Yellott, 1982). Following Williams (1985), we use the term Nyquist limit in this study to refer to the spatial frequency resolution limit corresponding to the mean sampling unit spacing for a given retinal area.

Naso-temporal asymmetry

Corresponding points in the far periphery of the nasal and temporal retina are not equally sensitive: beyond the optic nerve head the acuity limit in the nasal retina for both achromatic and chromatic stimuli is two to three times that in the temporal retina (see Fig. 5). For other visual tasks this difference is already quite well known: a naso-temporal retinal asymmetry has been reported for vernier acuity (Fahle & Schmid, 1988), binocular rivalry (Fahle, 1987), achromatic contrast sensitivity (Rovamo & Virsu, 1979), chromatic contrast sensitivity (Noorlander, Koenderink, Den Ouden & Edens, 1983) and orientation discrimination (e.g. Paradiso & Carney, 1988).

The pattern of asymmetry we observe for achromatic and chromatic stimuli cannot result from differences between cortical hemispheres as identical patterns of naso-temporal asymmetry occur for both right and left eyes.

Sites at which visual performance is limited

Previous studies have attempted to relate eccentricity- and meridional-dependent variations in visual resolution to the neural architecture of primate retina (e.g. Thibos *et al.* 1987*a*; Merigan & Katz, 1990). Both Merigan & Katz and Thibos *et al.* used an orientation discrimination protocol to measure peripheral visual acuity, the former in macaques and the latter in humans. Both studies compared their results with monkey retinal anatomy and both reach similar conclusions: measured acuities closely matched cone Nyquist frequencies out to 10 deg, but matched the Nyquist frequency of P ganglion cells at greater eccentricities. However, an orientation discrimination protocol may not yield an 'alias-free' measure of acuity. Williams & Coletta (1987) show that a resolution criterion based on orientation can produce acuity estimates as much as 1·5 times higher than the nominal Nyquist frequency of the underlying mosaic.

In this study, we also attempt to relate visual resolution to retinal architecture, but do so with two clear advantages. First, we compared our psychophysical measures of visual acuity to anatomical data from human eyes. Second, we went to some lengths to ensure that our measures of acuity were not affected by the detection of aliasing artifacts.

Spatial integration of light over the aperture of individual cones produces an effective blurring of the retinal image; the cone aperture acts as a low-pass filter (see Appendix for details). The extent of filtering will depend on the size of the 'effective cone aperture'. In the human retina, the cone inner segment functions as an optical wave guide, funnelling light into the smaller outer segment (e.g. Enoch, 1961). Thus, the effective aperture of a single cone is likely to be the cone's inner segment diameter near its maximum, which increases from 0·008 deg in the fovea to 0·029 deg at 40 deg eccentricity (C. A. Curcio, personal communication). In Fig. 5 we plot the cut-off spatial frequency of the modulation transfer function (MTF) for the inner segment aperture of individual cones at different eccentricities. Note that the limit of receptoral filtering far exceeds achromatic acuity in both central and peripheral vision.

For chromatic acuity, it is not appropriate to compare the aperture limitations for single cones. To encode a chromatic signal, a comparison between signals from a

minimum of two different cone types (such as L and M cones) is required. To determine the extent of receptoral filtering for chromatic stimuli, we calculated the MTF of cone doublets (see Appendix for details). In the fovea, the cut-off spatial frequency of a cone doublet (chosen as the first zero crossing of the MTF) is 57·7 cycles deg^{-1}, which exceeds chromatic acuity by a factor of 2·2. At 30 deg eccentricity, the cone doublet cut-off frequency exceeds chromatic acuity by a factor of about 6·0 in the nasal retina and 18·0 in the temporal retina. Thus, receptor–aperture blur is unlikely to pose any serious limitations to either achromatic or chromatic spatial vision.

Discrete spatial sampling by the cone mosaic could potentially limit spatial vision, due to aliasing. To avoid aliasing each cycle of a periodic waveform must be sampled by at least two sampling points. The Nyquist limit would be the spatial frequency corresponding to a sampling point beneath each bright bar (or red bar) and each dark bar (or green bar) of the waveform. There are potentially as many sampling points consisting of cone doublets as there are single cones, assuming each cone is connected to its nearest neighbour of opposite type and there are approximately equal numbers of M and L cones in a regular array. This being the case, there is no reason to think that the cone Nyquist limit for chromatic detection is any different to that for luminance detection. This allows us to compare the cone Nyquist limits plotted in Fig. 5 with both the achromatic and chromatic acuity measures.

For achromatic stimuli, our measures of foveal acuity approximate the limitations dictated by the sampling density of the cone mosaic. This is already so well known as to need no special discussion here (e.g. Williams, 1985). However, in the periphery achromatic acuity falls short of this limitation. The cone Nyquist limit matches achromatic acuity out to 5 deg, but beyond this the shape of the acuity–eccentricity function shows no dependence on cone density. At 50 deg the cone Nyquist limit and achromatic acuity are about an order of magnitude apart in each meridian. We conclude that beyond 5 deg eccentricity, receptoral sampling does not limit achromatic acuity. Further support for this claim comes from the fact that there is a significant naso-temporal asymmetry in achromatic acuity, yet the cone Nyquist limit is about the same in both hemifields.

For chromatic stimuli, our estimates of both foveal and peripheral acuity are substantially less than the cone Nyquist limit (Fig. 5). In the fovea, the cone Nyquist limit exceeds chromatic acuity by a factor of 2·2, and at 30 deg eccentricity, by a factor of 6·0 in the nasal retina and 18·0 in the temporal retina. We suggest therefore that receptoral sampling is not a determinant of chromatic acuity in either foveal or peripheral vision.

Peripheral visual resolution and ganglion cells

The acuity–eccentricity functions are qualitatively similar to the Nyquist frequency for ganglion cells, in that they reflect the naso-temporal asymmetry in ganglion cell density. Contrary to Thibos *et al.* (1987*a*) and Merigan & Katz (1990), however, we don't find an exact quantitative match. In the far periphery (> 20 deg), the ganglion cell Nyquist limit exceeds achromatic acuity by a factor of about two, and chromatic acuity by a factor of three or more (see Fig. 5). However, we cannot conclude from this that peripheral visual acuity is limited by a post-retinal process.

To begin with, the Nyquist limits plotted in Fig. 5 were derived from the density

measures on the population of ganglion cells as a whole, as human data is not yet available on the different classes of ganglion cells known to exist in primate retina (see Perry *et al.* 1984). It may be the case that the different psychophysical tasks used in this paper, direction discrimination of luminance-modulated patterns and

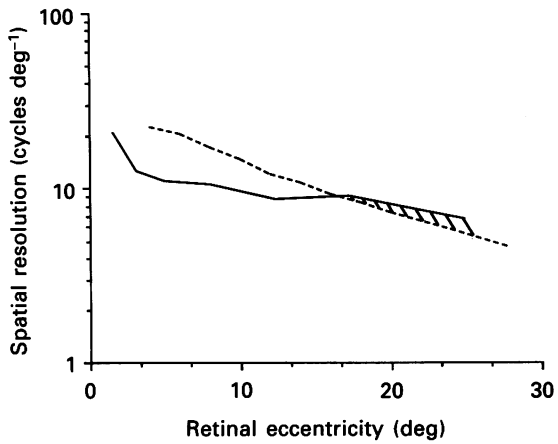

Fig. 6. Relationship between ganglion cell properties and retinal eccentricity in the Macaque monkey (data are for the temporal retina). The continuous line shows the spatial acuity of tonic ganglion cells (from Crook *et al.* 1988); the dashed line shows the Nyquist limits calculated from measurements of ganglion cell density (from Perry *et al.* 1984). The Nyquist limits were derived assuming a square array of cells and that one degree of visual angle corresponds to 0·25 mm in the monkey retina. In the peripheral visual field (beyond 15 deg) there is a region(indicated by the hatched area) where some ganglion cells respond to spatial frequencies greater than the ganglion cell Nyquist limit. In this region, aliasing phenomena may be expected.

chromatic detection of red–green patterns, are mediated by different subclasses of ganglion cells. This being the case, one would expect the Nyquist frequency for ganglion cells as a whole to exceed our acuity estimates.

Moreover, visual resolution may be limited by the spatial acuity of individual ganglion cells, as dictated by the extent of receptoral pooling. In this paper, we used alias-free measures of spatial acuity so as to allow a useful comparison with anatomical estimates of neural densities. However, alias-free measures of acuity could in principle be limited by either the sampling density or spatial acuity of ganglion cells. Information on the latter is not available for humans, but Crook *et al.* (1988) report such data for macaque monkey. In Fig. 6 we compare the spatial acuity of ganglion cells (from Crook *et al.*) with ganglion cell Nyquist limits (from Perry *et al.* 1984) at different eccentricities in the monkey retina. There is evidence to suggest that alias-free measures of acuity may be limited by the spatial acuity of individual ganglion cells in the near periphery (less than 15 deg), and by the sampling density of ganglion cells in the far periphery (see Fig. 6).

A similar situation may exist in the human retina, at least for the processing of achromatic stimuli. Spatial sampling artifacts are only observed under normal viewing conditions in human vision at eccentricities beyond about 20 deg (Anderson & Hess, 1990). Also, the sampling artifacts observed in human peripheral vision cannot be due to receptoral sampling, as they occur for spatial frequencies up to an

order of magnitude lower than that expected on the basis of measurements of human cone density (Thibos *et al.* 1987*a*; Anderson & Hess, 1990). Finally, there is a qualitative agreement between achromatic acuity and ganglion cell Nyquist limits in the human retina: the extent of asymmetry in achromatic acuity is substantially more marked along the horizontal meridian than along the vertical meridian (compare Figs 1 and 2), which is in accord with human ganglion cell density measurements (Curcio & Allen, 1990). We suggest that, beyond the optic nerve head, the spacing of ganglion cells may pose a fundamental limit on the spatial resolution of achromatic stimuli.

However, the sampling density of ganglion cells is unlikely to be a limiting factor for peripheral chromatic acuity. We can find no evidence for aliasing, and the acuity limit for detecting red–green gratings in peripheral vision is quite different to the limits expected on the basis of ganglion cell density. Also, the fact that chromatic acuity falls more rapidly with retinal eccentricity than achromatic acuity (see Fig. 5) provides evidence to suggest that different mechanisms are responsible for limiting achromatic and chromatic acuity. We conclude that either the spatial filtering properties of cone-opponent ganglion cells or post-retinal factors limit peripheral chromatic acuity.

APPENDIX

Optical transfer functions (OTFs) were calculated from measurements of foveal (Campbell & Gubisch, 1966) and peripheral (Jennings & Charman, 1981) line spread functions (LSFs). Foveal LSFs were measured with a 2·4 mm pupil, and peripheral LSFs with a 7·5 mm pupil. Maximum spatial frequency resolution was measured at the point where the contrast transmission of the OTF was 0%.

In addition to optical filtering, the circular aperture of individual cones will act as a low-pass filter. The modulation transfer function, M, of a single circular aperture is given by:

$$M = 2J_1(\pi vd)/(\pi vd),$$

where J_1 is a Bessel function of the first kind (order one), v is spatial frequency (cycles deg^{-1}), and d is cone diameter (deg) (from Snyder & Miller, 1977). This function is plotted in Fig. 7*A* for $d = 0{\cdot}008$ deg (continuous curve: inner segment diameter of foveal cones) and $d = 0{\cdot}029$ deg (dashed curve: inner segment diameter of cones at 40 deg eccentricity). For all calculations, we assumed that the cone inner segment aperture is circular and that one degree of visual angle corresponds to 0·29 mm in the human retina (e.g. Curcio *et al.* 1990). Human cone dimensions were provided by C. A. Curcio (personal communication). Following Miller & Bernard (1983), the first zero crossing of the modulation transfer function was chosen as a measure of the highest spatial frequency passed by the cone aperture and plotted in Fig. 5 as a function of retinal eccentricity.

Chromatic contrast detection requires a minimum of two cones of different type (e.g. Lennie & D'Zmura, 1988). The requirement of a cone pair will increase the extent of receptor–aperture blur. Applying the shift theorem (Bracewell, 1986), the modulation transfer function, M_2, of two adjacent circular apertures is given by:

$$M_2 = 2\cos(\pi vs)\,[2J_1(\pi vd)/(\pi vd)],$$

where s is the centre-to-centre spacing (deg) between the apertures. This function was evaluated for cones at various retinal locations. Figure 7*B* shows M_2 for a foveal cone doublet (continuous curve: $d = 0{\cdot}008$ deg; $s = 0{\cdot}0087$ deg) and for a cone doublet at 40 deg eccentricity (dashed curve: $d = 0{\cdot}029$ deg; $s = 0{\cdot}056$ deg). The first

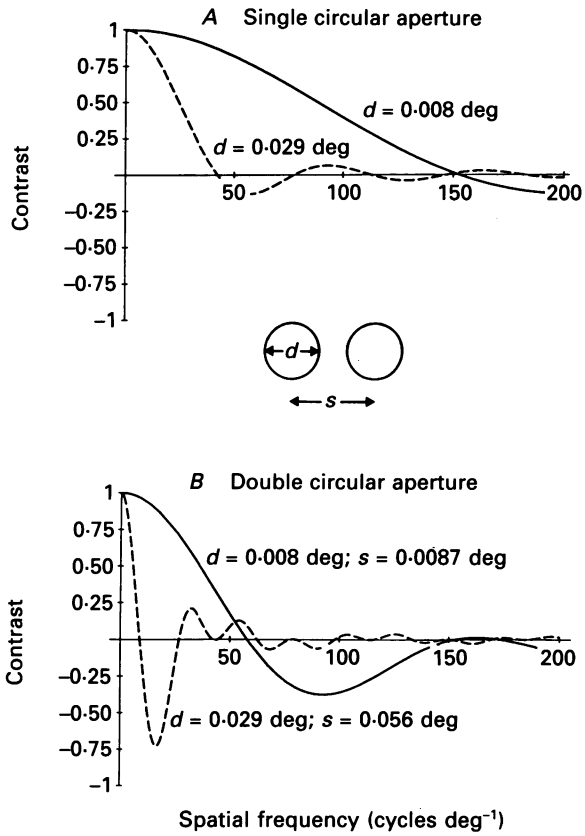

Fig. 7. *A*, modulation transfer function for a single circular aperture of diameter (d) equal to either 0·008 deg (foveal cone inner segment diameter; continuous line) or 0·029 deg (cone inner segment diameter at 40 deg eccentricity; dashed line). *B*, modulation transfer function for a pair of adjacent circular apertures: the continuous line is where each aperture has a diameter (d) of 0·008 deg and a centre-to-centre spacing (s) of 0·0087 deg; the dashed line is where each aperture has a diameter of 0·029 deg and a centre-to-centre spacing of 0·056 deg. See text for explanation.

zero crossing of the transform was chosen as the cut-off spatial frequency of each cone doublet. This criterion is arbitrary, though conservative, as spatial frequencies higher than this are passed (albeit with a $\pi/2$ phase shift) with significant contrast modulation (see Fig. 7*B*). Cut-off frequencies for cone doublets ranged from 57·7 cycles deg^{-1} in the fovea to 8·9 cycles deg^{-1} at 40 deg eccentricity.

Cone and ganglion cell spacing were calculated from anatomical measures of their respective densities in cells mm^{-2}. We assumed a square array of cells of density D cells per unit area. Cell spacing (min of arc) is given by $S = [(1/\sqrt{D})\ (60/0{\cdot}29)]$ and the Nyquist limit (NL, cycles deg^{-1}), plotted in Fig. 5, is $\mathrm{NL} = 60/2S$. Of course,

alternative packing arrangements can be assumed. For the human fovea, a hexagonal packing arrangement seems appropriate (e.g. Williams, 1985), although this arrangement yields resolution values that differ by only 5–7 % to those predicted using a square array. Packing arrangement of cones and ganglion cells is less regular in the periphery and as there is no evidence to assume one type of packing arrangement over another, we adopted the simplest strategy at this stage.

Foveal ganglion cell density had to be estimated. Several factors make it difficult to quantify foveal ganglion cell density, including the differentiation of ganglion cells from displaced amacrine cells and the fact that there is a spatial offset between foveal cone inner segments and ganglion cells due to cone fibres (see Wassle, Grunert, Rohrenbeck & Boycott, 1989; Curcio & Allen, 1990). Recent estimates of the cone/ganglion cell ratio at the foveal centre range from 1/2 to 1/3·34 (Wassle *et al.* 1989; Curcio & Allen, 1990). For Fig. 5, we assumed a foveal cone/ganglion cell ratio of 1/2.

We thank Dr Christine Curcio for providing anatomical data on the human retina and Dr Fred Kingdom for many helpful discussions. S.J.A. held the William E. Buck Memorial Post-doctoral Fellowship from St John's College, Cambridge. Some of these results were presented at the Annual Spring Meeting of the Association for Research in Vision and Ophthalmology, Sarasota, Florida, April, 1989.

REFERENCES

ANDERSON, S. J. & BURR, D. C. (1987). Receptive field size of human motion detection units. *Vision Research* **27**, 621–635.

ANDERSON, S. J. & HESS, R. F. (1990). Post-receptoral undersampling in normal human peripheral vision. *Vision Research* **30**, 1507–1515.

BANKS, M. S., GEISLER, W. S. & BENNETT, P. J. (1987). The physical limits of grating visibility. *Vision Research* **27**, 1915–1924.

BRACEWELL, R. N. (1986). *The Fourier Transform and its Applications*, 2nd edn (revised). McGraw-Hill, New York.

BURR, D. C. & ROSS, J. (1982). Contrast sensitivity at high velocities. *Vision Research* **22**, 479–484.

CAMPBELL, F. W. & GUBISCH, R. W. (1966). Optical quality of the human eye. *Journal of Physiology* **186**, 558–578.

COLETTA, N. J., WILLIAMS, D. R. & TIANA, C. L. M. (1990). Consequences of spatial sampling for human motion perception. *Vision Research* **30**, 1631–1648.

CROOK, J. M., LANGE-MALECKI, B., LEE, B. B. & VALBERG, A. (1988). Visual resolution of macaque retinal ganglion cells. *Journal of Physiology* **396**, 205–224.

CURCIO, C. A. & ALLEN, K. A. (1990). Topography of ganglion cells in human retina. *Journal of Comparative Neurology* **300**, 5–25.

CURCIO, C. A., SLOAN, K. R., KALINA, R. E. & HENDRICKSON, A. E. (1990). Human photoreceptor topography. *Journal of Comparative Neurology* **292**, 497–523.

ENOCH, J. (1961). Nature of the transmission of energy in the retinal receptors. *Journal of the Optical Society of America* **51**, 1122–1126.

FAHLE, M. (1987). Naso-temporal asymmetry of binocular rivalry. *Investigative Ophthalmology and Visual Science* **28**, 1016–1017.

FAHLE, M. & SCHMID, M. (1988). Naso-temporal asymmetry of visual perception and of the visual cortex. *Vision Research* **28**, 292–300.

FRENCH, A. S., SNYDER, A. W. & STAVENGA, D. G. (1977). Image degradation by an irregular retinal mosaic. *Biological Cybernetics* **27**, 229–233.

GOTZ, K. G. (1964). Optomotorische Untersuchung des visuellen Systems einiger Augenmutanten der Fruchtfliege Drosophila. *Kybernetik* **2**, 77–92.

HESS, R. F., MULLEN, K. T. & ZRENNER, E. (1989). Human photopic vision with only short wavelength cones: post-receptoral properties. *Journal of Physiology* **417**, 151–172.

JENNINGS, J. A. M. & CHARMAN, W. N. (1981). Off-axis image quality in the human eye. *Vision Research* **21**, 445–455.

KELLY, D. H. (1983). Spatiotemporal variation of chromatic and achromatic contrast thresholds. *Journal of the Optical Society of America* **73**, 742–750.

LENNIE, P. & D'ZMURA, M. (1988). Mechanisms of color vision. *CRC Critical Reviews in Neurobiology* **3**, 333–400.

LINDSEY, D. T. & TELLER, D. Y. (1990). Motion at isoluminance: Discrimination/detection ratios for moving isoluminant gratings. *Vision Research* **30**, 1751–1761.

LOW, F. N. (1951). Peripheral visual acuity. *Archives of Ophthalmology* **45**, 80–99.

MILLER, W. H. & BERNARD, G. D. (1983). Averaging over the foveal receptor aperture curtails aliasing. *Vision Research* **23**, 1365–1369.

MERIGAN, W. H. & KATZ, L. M. (1990). Spatial resolution across the macaque retina. *Vision Research* **30**, 985–991.

MULLEN, K. T. (1985). The contrast sensitivity of human colour vision to red–green and blue–yellow chromatic gratings. *Journal of Physiology* **359**, 381–400.

MULLEN, K. T. (1991). Colour vision as a post-receptoral specialization of the central visual field. *Vision Research* **31**, 119–130.

NOORLANDER, C., KOENDERINK, J. J., DEN OUDEN, R. J. & EDENS, B. W. (1983). Sensitivity to spatiotemporal colour contrast in the peripheral visual field. *Vision Research* **23**, 1–11.

OSTERBERG, G. (1935). Topography of the layer of rods and cones in the human retina. *Acta Ophthalmologica*, suppl. 6, 1–103.

PARADISO, M. A. & CARNEY, T. (1988). Orientation discrimination as a function of stimulus eccentricity and size: Nasal/temporal retinal asymmetry. *Vision Research* **28**, 867–874.

PERRY, V. H., OEHLER, R. & COWEY, A. (1984). Retinal ganglion cells that project to the dorsal lateral geniculate nucleus in the macaque monkey. *Neuroscience* **12**, 1101–1123.

POLYAK, S. L. (1957). *The Vertebrate Visual System*. University of Chicago Press, Chicago.

ROBSON, J. G. (1966). Spatial and temporal contrast sensitivity functions of the visual system. *Journal of the Optical Society of America* **56**, 1141–1142.

ROBSON, J. G. & GRAHAM, N. (1981). Probability summation and regional variation in contrast sensitivity across the visual field. *Vision Research* **21**, 409–418.

ROVAMO, J. & VIRSU, V. (1979). An estimation and application of the human cortical magnification factor. *Experimental Brain Research* **37**, 495–510.

SMITH, R. A. & CASS, P. F. (1987). Aliasing in the parafovea with incoherent light. *Journal of the Optical Society of America* **4**, 1530–1534.

SNYDER, A. W. & MILLER, W. H. (1977). Photoreceptor diameter and spacing for highest resolving power. *Journal of the Optical Society of America Letters* **67**, 696–698.

THIBOS, L. N., CHENEY, F. E. & WALSH, D. J. (1987*a*). Retinal limits to the detection and resolution of gratings. *Journal of the Optical Society of America* **4**, 1524–1529.

THIBOS, L. N., WALSH, D. J. & CHENEY, F. E. (1987*b*). Vision beyond the resolution limit: aliasing in the periphery. *Vision Research* **27**, 2193–2197.

WASSLE, H., GRUNERT, U., ROHRENBECK, J. & BOYCOTT, B. B. (1989). cortical magnification factor and the ganglion cell density of the primate retina. *Nature* **341**, 643–646.

WERTHEIM, T. (1894). Ueber die indirekte Sehscharfe. *Zeitschrift fur Psychologie und Physilogische Sinnesorgen* **7**, 172–189.

WILLIAMS, D. R. (1985). Aliasing in human foveal vision. *Vision Research* **25**, 195–205.

WILLIAMS, D. R. & COLETTA, N. J. (1987). Cone spacing and the visual resolution limit. *Journal of the Optical Society of America* **4**, 1514–1523.

WILLIAMS, D. R., COLLIER, R. J. & THOMPSON, B. J. (1983). Spatial resolution of the short-wavelength mechanism. In *Colour Vision, Physiology and Psychophysics*, ed. MOLLON, J. D. & SHARPE, L. T., pp. 487–503. Academic Press, London.

YELLOTT, J. I. (1982). Spectral analysis of spatial sampling by photoreceptors: topological disorder prevents aliasing. *Vision Research* **22**, 1205–1210.

ZEKI, S. M. (1978). Uniformity and diversity of structure and function in rhesus monkey prestriate visual cortex. *Journal of Physiology* **277**, 273–290.